Infliximab was given intravenously over 2 h at a dose of 5 mg/kg on 0, 2, and 6 weeks, with follow-up treatments every 7–8 weeks depending on clinical symptoms. The patient was monitored regularly throughout the infliximab treatment.

Results

Case

The patient was born to unrelated Japanese parents after an uncomplicated pregnancy of 41 weeks. There was no history of any first-degree relative diagnosed with incontinentia pigmenti. On the first day after birth, he presented high fever with a markedly increased white blood cell count ($40\times10^3/\mu L$) and was treated successfully with antibiotics. He has had a history of recurrent, severe infections including varicella at 3 months of age, penicillin-resistant *Streptococcus pneumoniae* meningitis at 6 months of age, and zoster at 8 months of age. Persistent diarrhea was also observed.

He was introduced to our hospital at 8 months of age for examination of his immunological status. On admission, he showed a marked increase in both white blood cells ($31.9\times10^3/\mu L$) and platelets ($872\times10^3/\mu L$). Peripheral blood T cell count was decreased (CD3-positive cells, 25.8%), and B cell count was highly increased (CD20-positive cells,: 69.2%). PHA induced a normal proliferation response of T cells, and concentrations of immunoglobulins were within the normal range except IgD (less than 0.2 mg/dL). Natural killer cell activity was markedly impaired. Superoxide-generating ability from neutrophils was intact. LPS-induced TNFα production from patient's PBMC was impaired (Fig. 1a). Interferon (IFN) γ-producing lymphocytes were also reduced apparently at 8 months of age (Table I). All the genes involving in the IL-12 signal pathway, including *IL12RB1*, *IL12RB2*, *JAK2*, and *STAT4* were sequenced, but no mutations were found (data not shown). Surprisingly, both IFNγ-producing T cells and natural killer cells had expanded significantly by 11 months of age (Table I). In addition, we observed that he had ectodermal dysplasia including anhidrosis and conical teeth (Supplementary Fig. 1). A skin biopsy revealed the absence of eccrine sweat glands. When he was 3 years old, a G505C (A169P) missense mutation in his *IKBKG* gene was confirmed and diagnosed as X-EDA-ID. His mother was a carrier. An expression of mutant NEMO protein was not markedly

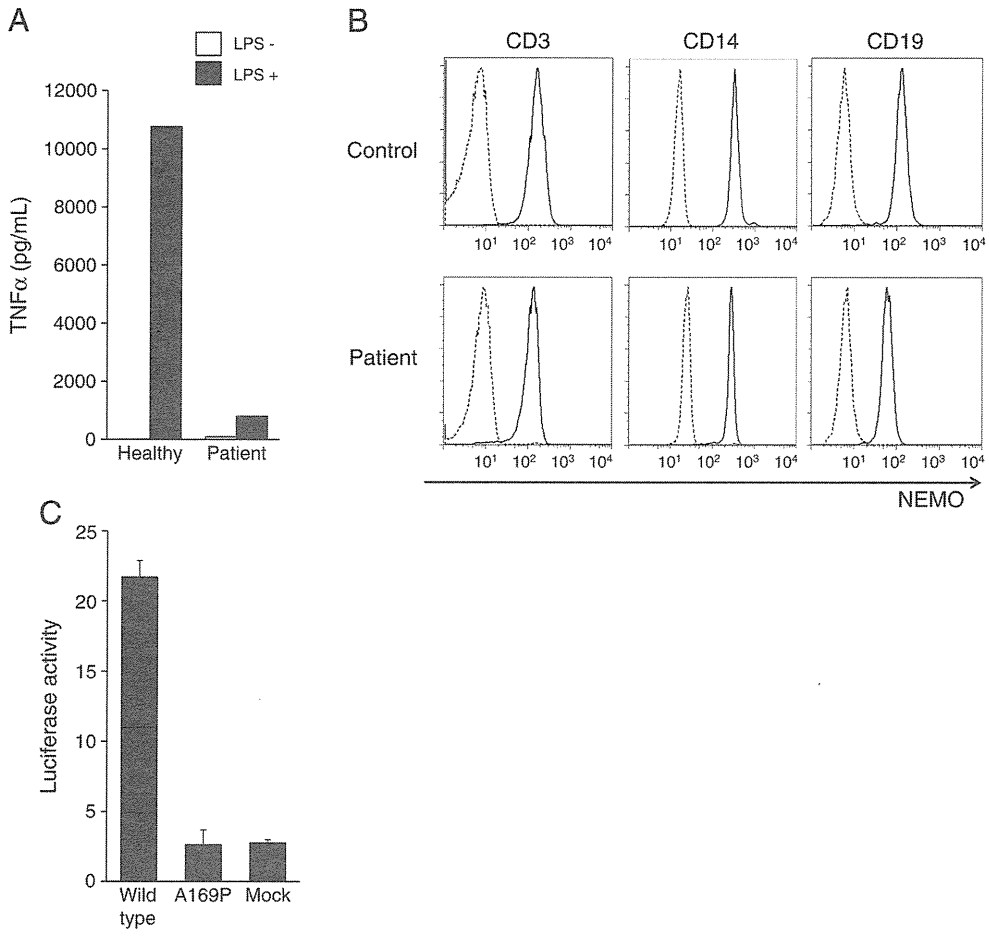

Fig. 1 Analysis of mutant NEMO protein. **a** Reduced production of TNFα from LPS-stimulated PBMCs. PBMCs from our patient and healthy volunteer were stimulated with LPS (1 μg/mL). **b** Analysis of NEMO protein expression using flow cytometry. Intracellular NEMO protein in PBMCs from the patient was not reduced markedly. **c** The result of NEMO-NF-κB luciferase reporter assay. The activity of mutant NEMO in the patient was almost defective. Mock vectors and wild-type NEMO were used as controls. *Error bars* indicate SD

Table I Proportion of IFNγ-expressing T and NK cells in the patient

Age	$IFN\gamma^+/IL\text{-}4^-$		
	CD4 (%)	CD8 (%)	CD56 (%)
8 months	1.14	8.83	2.00
11 months	3.18	70.40	66.29
3 years 11 months	11.89	65.48	82.79
Healthy control	15	60–80	80–90

reduced by flow cytometer (Fig. 1b), but the activity of mutant NEMO was almost defective which was confirmed by a mutant NEMO-NF-κB luciferase reporter assay (Fig. 1c). He has been prescribed prophylactic cotrimoxazole before and after the diagnosis.

He presented with chest pain, erythema, polyarthritis, continuous high fever refractory to antibiotics, and marked elevation of C-reactive protein (7.4 mg/dL) at 4 years of age. Autoantibodies such as anti-centromere antibody were detected transiently. Chest computed tomography revealed multiple nodular shadows resembling bronchiolitis obliterans organizing pneumonia. The repertoire of T cell receptor showed high expression of limited Vβ subsets (Supplementary Fig. 2). Combination therapy using corticosteroids, cyclosporine A, and methotrexate was effective and was continued to control his symptoms.

Severe abdominal pain and intractable frequent diarrhea recurred when the corticosteroid dose was reduced, and he presented perianal fistula at 8 years of age. A mild elevation was observed in both erythrocyte sedimentation rate and C-reactive protein under the preceding immunosuppressive treatments (Table II). No significant pathogen was detected by stool culture and the use of antibiotics and antifungal drugs resulted in no improvement in clinical symptoms.

Endoscopic and Microscopic Findings of the Colon

Colonic endoscopy revealed many polyp-like lesions with mucosal redness and edema at the sigmoid/descending junction (Fig. 2). A longitudinal ulcerative lesion found in the sigmoid colon was suggestive of Crohn's disease. Passing the endoscope beyond these obstructive clusters of polyps was difficult; therefore, we could not observe the upper part of the colon. Neither stenosis nor ulcer formation was observed by intestinal radiocontrast analysis.

Histopathological examination of the colonic biopsied specimens showed diffuse lymphoplasmacytic infiltration, superficial edema, and hyperemia in lamina propria. Foamy cells and some eosinophils were also seen (Fig. 3a, b). No definite neutrophilic infiltration, crypt abscesses, or granulomatous lesions were observed. Cultures from biopsied specimens yielded neither bacterial nor fungal growth.

Immunohistochemical staining revealed predominant infiltration of CD79a-positive, plasma cells in the lamina propria. Infiltration of CD68-positive macrophages and CD3-positive T cells was also observed (Fig. 3c–g).

Detection of TNFα-Producing Cells in the Lamina Propria and Peripheral Blood

To investigate the possibility that TNFα blockade therapy can ameliorate inflammatory colitis as well as NEMO-deficient mice as suggested by previous analysis [15], we analyzed TNFα-producing mononuclear cells in the lamina propria in the colon of our patient. Immunohistochemical staining showed abundant TNFα in infiltrated mononuclear cells in the lamina propria (Fig. 3h) which would be associated with progression of inflammatory colitis.

We also analyzed TNFα-producing T cells and monocytes in the peripheral blood (Fig. 4a). The majority (72.49%) of CD4-positive T cells in our patient expressed intracellular TNFα, while 40% to 70% of CD4-positive T cells expressed TNFα in adults with IBD in our study. Forty-eight percent of CD8-positive T cells in our patient expressed TNFα. CD14-positive monocytes from our patient expressed small amounts of intracellular TNFα after LPS stimulation, while similarly treated CD14-positive cells from healthy subjects expressed abundant TNFα (Fig. 4b).

Reversion Analysis

Nishikomori et al. reported that in an X-EDA-ID patient, the mutation had been reverted to the normal state in IFNγ-

Table II Laboratory data on admission (8 years old)

WBC	13,600/μL	CD3	76.2%	IgG	790 mg/dL
Neutrophils	10,200/μL	CD4	22.2%	IgA	666 mg/dL
Lymphocytes	1,632/μL	CD8	58.3%	IgM	71 mg/dL
Monocytes	952/μL	CD19	4.8%	IgD	<0.6 mg/dL
Hemoglobin	12.0 g/dL	CD20	3.8%	C3	134 mg/dL
Platelets	84.7×10^4/μL	CD16	0.5%	C4	46 mg/dL
		CD56	33.6%	CH50	56 U/mL
		HLA-DR	26.5%	ESR	43 mm/h

WBC white blood cell, *CH50* total complement activity, *ESR* erythrocyte sedimentation rate

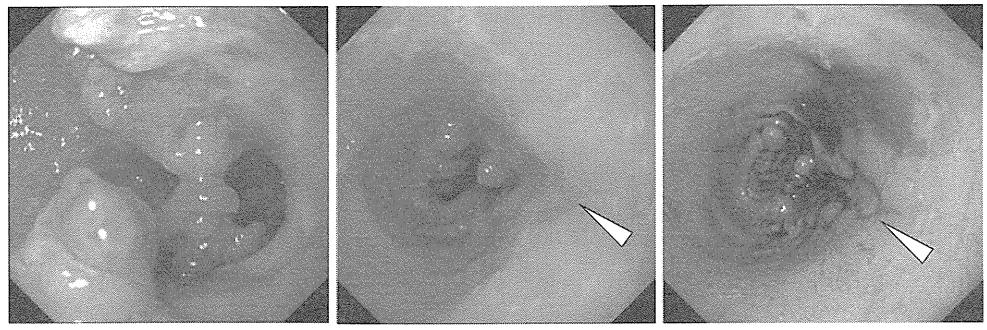

Fig. 2 Findings of colonoscopy performed before initial treatment with infliximab. Colonoscopy revealed polyp-like lesions with mucosal redness and edema at the sigmoid/descending junction (*left panel*). A longitudinal ulcer (*arrowhead*) was found in the sigmoid colon (*center panel*). Same segment as in the *center panel* after indigo carmine dye (*right panel*)

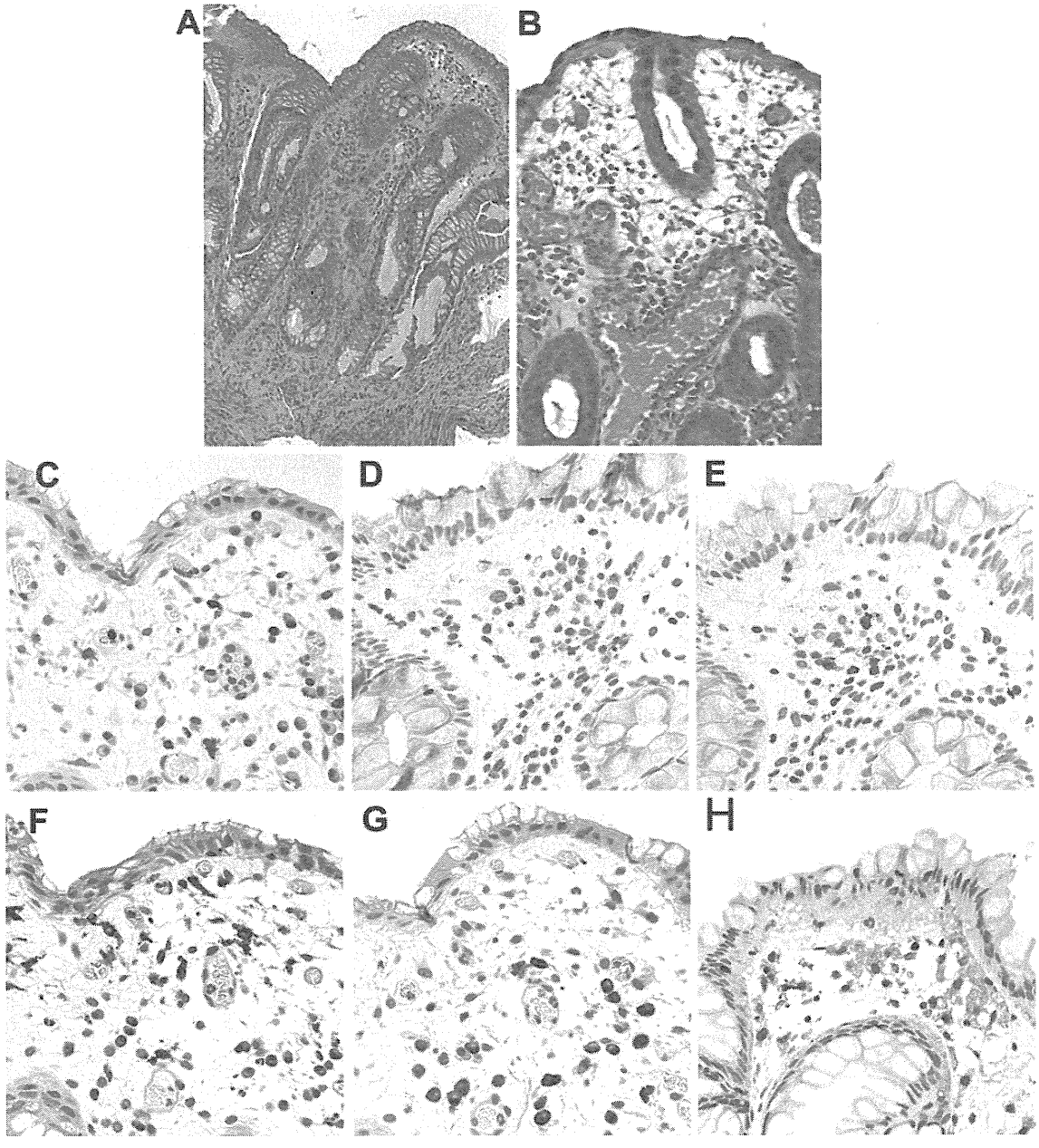

Fig. 3 Microscopic findings of affected colonic specimens. **a**, **b** Hematoxylin and eosin staining. **a** and **b** are low-power field and high-power field views, respectively. **c**–**h** Staining profiles of cellular surface antigens: **c** CD3ε, **d** CD4, **e** CD8, **f** CD68, and **g** CD79a. **h** Staining with anti-human TNFα antibody

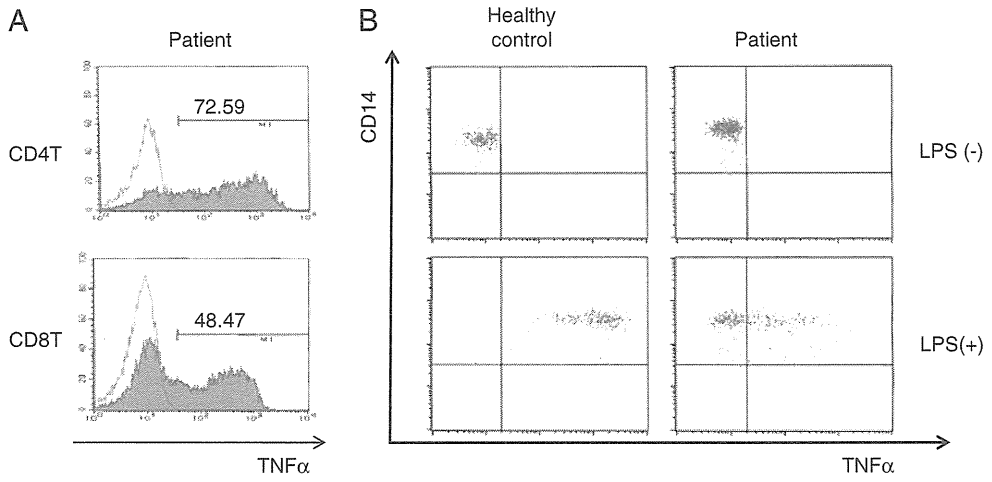

Fig. 4 Analysis of TNFα-producing mononuclear cells in peripheral blood. **a** TNFα-expressing T cells increased markedly before infliximab treatment. PBMCs were stimulated with ionomycin and PMA for 4 h in the presence of brefeldin A then stained for intracellular TNFα. For FACS analysis, gates were set on lymphocytes according to forward and side scatter properties. Representative histograms of TNFα expression in stimulated (*solid histograms*) or unstimulated (*black line histograms*) T cells. The proportion of TNFα-positive CD4-positive T cells in adult IBD patients is 40–70%. **b** The percentage of TNFα-positive monocytes was examined. Cells from our patient and healthy volunteer were incubated with or without LPS for 4 h in the presence of brefeldin A. Monocytes were identified by CD14. Approximately 50% of stimulated monocytes produced a small amount of TNFα

expressing T cells [18]. Our patient showed expansion of IFNγ-expressing T cells during infancy and an increase in TNFα-producing T cells at that time. We hypothesized that the A169P mutation in the *IKBKG* gene had been reverted to wild type and that the reverted T cells had expanded in our patient. Indeed, before initiating infliximab treatments, reversion mutation was detected in 23/67 (34%) from non-stimulated PBMCs (Table III). At 24 months after the initiation, reversion mutation was detected in both messenger RNA (mRNA) and genomic DNA from lymphocytes stimulated with PHA and IL-2 for 10 days, whereas only mutated mRNA was identified from non-stimulated lymphocytes (Fig. 5). Reverted mRNA was observed in CD3-positive T cells. Sex chromosome analysis with fluorescent in situ hybridization revealed no maternal cells and therefore graft-versus-host disease secondary to maternal–fetal transfusion was unlikely. These findings suggest that reverted T cells activated NF-κB in response to growth signals and had a growth advantage over mutant cells.

Table III Frequency of reverted clones before and after initiation of infliximab treatments

	Before	After 12 months	After 24 months
PBMCs	23/67 (34%)	nd	2/6 (33%)[a]
CD3	nd	3/16 (19%)	nd
CD14	nd	0/19 (0%)	nd
CD19	nd	0/47 (0%)	nd

nd not done

[a] A result using stimulated mononuclear cells

Reverted T cells decreased with repeated administrations of anti-TNFα monoclonal antibody. In contrast, CD14-positive monocytes and GM-CSF-induced monocyte-derived dendritic cells had no reversion (Table III).

Anti-TNFα Treatment Improved NEMO Colitis

We initially treated NEMO colitis with high dose corticosteroid therapy (2 mg/kg prednisolone, daily) (Fig. 6). However, steroid therapy did not improve clinical symptoms and resulted in compression fracture in the thoracic spine from corticosteroid-induced osteoporosis.

The increase in TNFα-producing T cells suggested the possibility that TNFα blockade therapy would be an effective treatment for the intractable NEMO colitis. After confirming the absence of severe bacterial or mycobacterial infection, we initiated administration of the chimeric anti-TNFα monoclonal antibody, infliximab, to our patient.

Soon after the first infusion of infliximab, abdominal pain disappeared and his appetite recovered. Frequency of diarrhea decreased as administrations of infliximab were repeated (Fig. 6). Colonoscopy after his third administration showed mild improvement of both mucosal redness and edema (Fig. 7a). These mucosal inflammatory findings had almost disappeared after 1-year treatment with infliximab, although polyp-like lesions remained (Fig. 7b).

The proportion of TNFα-producing cells in CD4-positive and CD8-positive T cells markedly decreased by his third infliximab infusion (from 72.6% to 26.7% in CD4-positive T cells and from 48.5% to 23.1% in CD8-positive T cells), and reduction of TNFα-producing cells was

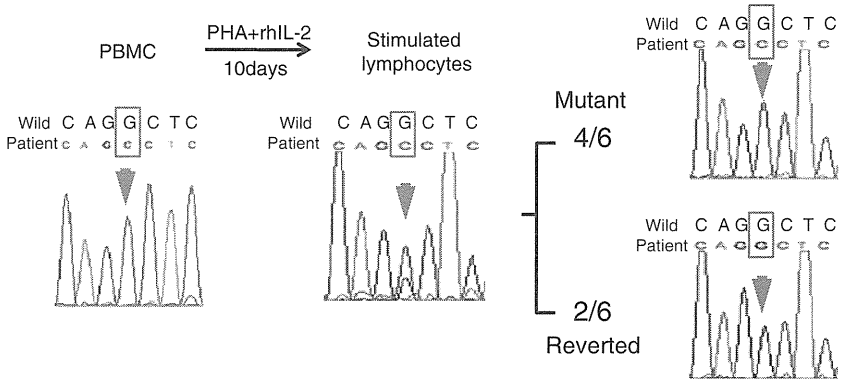

Fig. 5 Reversion analysis of cDNA of gene encoding NEMO isolated from mononuloclear cells after 24 months of infliximab treatment. PBMC was obtained from our patient and incubated with PHA and IL-2 for 10 days. Direct sequence for mRNA encoding NEMO was performed using PBMC and the stimulated mononuclear cells. Before stimulation, no reverted mononuclear cells were detected. After PHA and IL-2 stimulation, reverted mononuclear cells apparently increased. Subcloning of cDNA from stimulated cells showed that two of six cells had reversion of mutation in the gene

associated with improvement of clinical symptoms (Fig. 6). Administration of cyclosporine A was discontinued by the eighth infliximab treatment, and corticosteroid was reduced and then discontinued by the tenth infliximab infusion.

Our patient had one serious adverse event, pneumonia, after his fourth administration of infliximab. *Campylobacter jejuni* was isolated from his blood culture at that time. He was successfully treated with antibiotics and infliximab administration was resumed after confirming resolution of pneumonia. He has been treated safely for more than 2 years with regular administrations of infliximab (once every 7–8 weeks). Neither mycobacterial infections nor severe infusion reactions have been observed.

Discussion

Our patient showed immunodeficiency with very low IFNγ-production during his younger years as shown in Table I and suffered from many opportunistic infections (Zoster virus infection, penicillin-resistant *Streptococcus pneumoniae* meningitis, and other undetermined infections). A novel missense mutation, A169P, in the first coiled-coil domain resulted in defective NEMO function (Fig. 1) and was responsible for recurrent severe infections. However, he later suffered from autoimmune diseases at 4 years of age (bronchiolitis obliterans organizing pneumonia, severe arthritis, and vasculitis) and severe chronic inflammatory colitis at 8 years. Based on the facts that, in the mice model, TNFα played a major role in the pathogenesis of NEMO colitis [15], and that, in our patient, TNFα-producing mononuclear cells in the peripheral blood were markedly increased (Fig. 4a), infliximab was employed for the patient's treatment. This treatment led to improvement in his symptoms and colonoscopic findings for 2 years.

Increases in TNFα-producing cells similar to that seen in other IBD [19] were detected (Fig. 4). We confirmed G/C

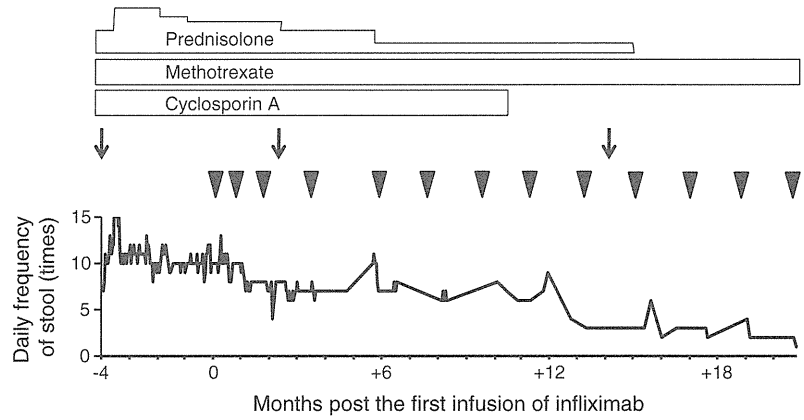

TNF+/CD4T(%)	72.6	26.7	38.0	45.7	52.4	32.7
TNF+/CD8T(%)	48.5	23.1	27.5	37.7	44.4	N.D.

Fig. 6 Clinical course of NEMO colitis after infliximab treatment in our patient. Colonoscopy (*arrows*), administrations of infliximab (*arrowheads*), and other immunosuppressive drugs (*bars*) are indicated. Daily frequency of stools (times) is graphed at the *center*. Changes in the proportion of TNFα-producing T cells in CD4-positive and CD8-positive cells are also indicated at the *bottom*

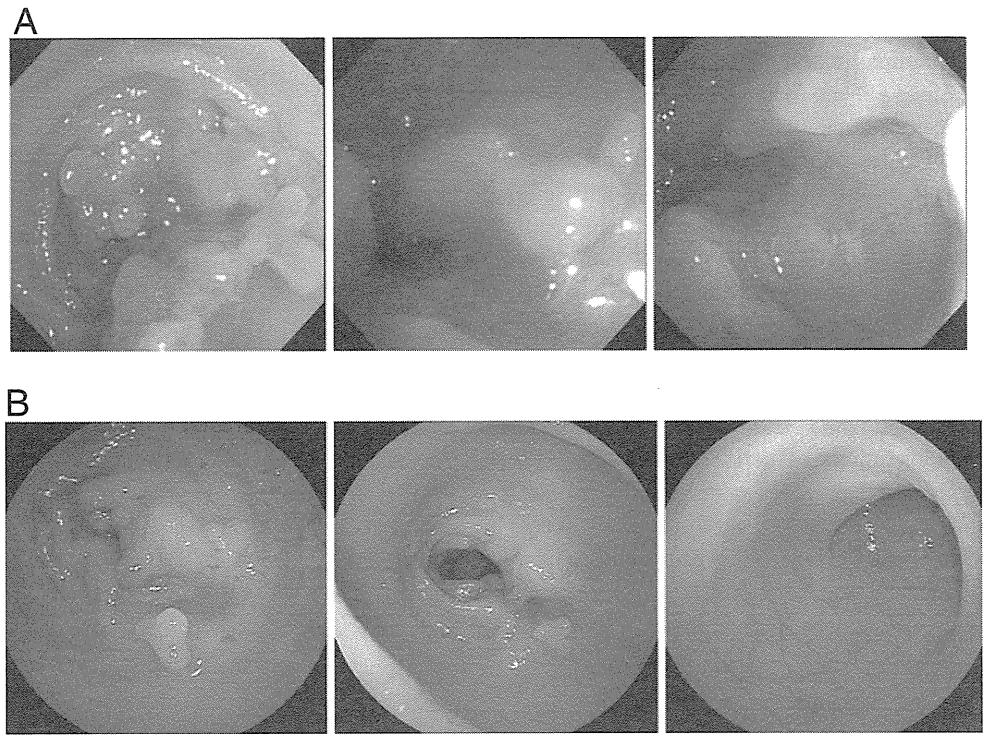

Fig. 7 Findings of colonoscopy after infliximab treatment. **a** Colonoscopy performed after the third infliximab treatment. Mild improvement was observed. Both mucosal redness and edema decreased. However, polyp-like lesions remained. At this point, the patient showed neither abdominal pain nor watery diarrhea. **b** Colonoscopy after 1-year treatment. Almost no mucosal redness or edema. A clear vascular pattern was also observed. Inflammatory polyps could still be found

reversion in T cells after co-stimulation with PHA and IL-2 before and even after infliximab therapy (Table III and Fig. 5). Reversion mosaicism has been reported in primary immunodeficiencies such as X-linked severe combined immunodeficiency [20, 21], adenosine deaminase deficiency [22], *RAG1* deficiency [23], and Wiskott–Aldrich syndrome [24]. Most of these patients reduced the frequency of severe infections and showed survival for longer periods. Our patient also had very few episodes of severe infection after expansion of IFNγ-producing peripheral blood mononuclear cells, contrary to increased susceptibility to diverse pathogens in X-EDA-ID [5, 25]. However, none of the patients with reversion mosaicism involving reverted T cells developed IBD other than X-EDA-ID. Our patient and patients with Omenn's syndrome [21, 23] developed systemic inflammatory conditions and exhibited a restricted TCR repertoire. In our patient, oligoclonal expansion of reverted T cells caused impairment of immune regulation.

According to the report by Nenci et al. in a murine model of intestinal epithelium-specific NEMO deficiency, intestinal epithelial cells exhibit increased sensitivity to TNFα-induced apoptosis and cause disruption of the epithelial barrier if mucosal immune cells have normal immune functions and produce proinflammatory cytokines [15]. They also showed that an additional TNF receptor-1 knockout ameliorated this intestinal inflammation [15]. The pathogenesis of severe colitis in the mouse model seems to be similar to that of our patient. Specifically, NEMO-deficient intestinal epithelium was damaged by TNFα produced from both T cells and macrophages in the lamina propria (shown in Fig. 3c–e, h), and anti-TNFα antibody suppressed progression of intestinal inflammation. Although reversion in peripheral blood monocytes was not confirmed after culture with GM-CSF and analysis of TNFα expression after LPS stimulation, submucosal and peripheral macrophages produced a fair amount of TNFα detectable by immunohistochemistry and flow cytometry (Figs. 3 and 4). Production of TNFα from lamina propria macrophages may be augmented by IFNγ released from reverted T cells.

In addition to the amelioration of clinical symptoms and colonic mucosal inflammation, in our patient, TNF blockade therapy restored his dry skin with thick epidermis to moderately moist skin of normal thickness. Nenci et al. described in another paper using the epidermis-specific NEMO-deficient mice that mice showed severe skin inflammation with thick epidermis and predominant infiltration of inflammatory cells and showed further that an additional knockout of TNFR1 suppressed the inflammatory condition [26]. We postulate that TNFα is also a key cytokine in the pathogenesis of inflammation in diverse epithelial tissues and that infliximab treatment suppresses the TNFα-mediated inflammatory response by inducing apoptosis of TNFα-producing cells [27]. In fact, the patient's peripheral blood TNFα-producing cells reduced along with the improvement of clinical symptoms, and this reduction provided an available marker to assess inflammatory status. Reverted cells in peripheral blood also decreased after repeated anti-TNFα antibody administrations. Unfortunately, we could not obtain consent for re-biopsy so we could not

confirm a vulnerability for apoptosis of intestinal epithelium and lamina propria after the treatment.

Since patients with X-EDA-ID were well known to have increased susceptibility to mycobacterium, and in addition, anti-TNFα monoclonal antibody indeed caused infection-related deaths in a few patients with inflammatory colitis associated with primary immunodeficiencies [28–30], the side effects of anti-TNFα monoclonal antibody treatment should be paid attention to, especially, mycobacterial infections. Before infliximab treatment, we confirmed the absence of active mycobacterial infections by culture tests for mycobacterium including atypical mycobacteria, laboratory examinations, and chest radiographs. He also has no history of Bacillus Calmette-Guérin immunization. Although the patient experienced bacterial pneumonia after his third infliximab infusion, he has not suffered from severe infections for several years. This may be because of the patient's mosaicism of mutated and reverted cells. The risks concerning severe infections and oncogenic effects [31–33] should be considered before employing infliximab for NEMO colitis.

Conclusion

Reversion of mutation in T cells contributes to the pathogenesis of mucosal immunity in NEMO-deficient patients. Moreover, treatment with anti-TNFα monoclonal antibody therapy can improve the symptoms of the disease by both preventing exposure of the mucosa to TNFα and reducing the number of T cells carrying the reverted gene. Anti-TNFα monoclonal antibody therapy provi[illegible] a promising treatment for intractable NEMO colitis.

Acknowledgments We profoundly thank for Dr. Kazuko Uno of the Louis-Pasteur Medical Research Center in Japan for support of our experiments and Dr. Maiko Kai and Dr. Naoki Karasawa1 for their warm care of patients. This study was supported by a Grant-in-Aid for Scientific Research from the Ministry of Education, Culture, Sports, Science and Technology, Japan.

Conflict of Interests The authors declare no competing financial interests.

References

1. Zonana J, Elder M, Schneider L, et al. A novel X-linked disorder of immune deficiency and hypohidrotic ectodermal dysplasia is allelic to incontinentia pigmenti and due to mutations in IKK-gamma (NEMO). Am J Hum Genet. 2000;67:1555–62.
2. Döffinger R, Smahi A, Bessia C, et al. X-linked anhidrotic ectodermal dysplasia with immunodeficiency is caused by impaired NF-kappaB signaling. Nat Genet. 2001;27:277–85.
3. Jain A, Ma CA, Liu S, et al. Specific missense mutations in NEMO result in hyper-IgM syndrome with hypohydrotic ectodermal dysplasia. Nat Immunol. 2001;2:223–8.
4. Orange JS, Brodeur SR, Jain A, et al. Deficient natural killer cell cytotoxicity in patients with IKK-gamma/NEMO mutations. J Clin Invest. 2002;109:1501–9.
5. Orange JS, Jain A, Ballas ZK, et al. The presentation and natural history of immunodeficiency caused by nuclear factor kappaB essential modulator mutation. J Allergy Clin Immunol. 2004;113:725–33.
6. Pai S, Levy O, Jabara H, et al. Allogeneic transplantation successfully corrects immune defects, but not susceptibility to colitis, in a patient with nuclear factor-kappaB essential modulator deficiency. J Allergy Clin Immunol. 2008;122:1113–1118.e1111.
7. Tono C, Takahashi Y, Terui K, et al. Correction of immunodeficiency associated with NEMO mutation by umbilical cord blood transplantation using a reduced-intensity conditioning regimen. Bone Marrow Transplant. 2007;39:801–4.
8. Mancini AJ, Lawley LP, Uzel G. X-linked ectodermal dysplasia with immunodeficiency caused by NEMO mutation: early recognition and diagnosis. Arch Dermatol. 2008;144:342–6.
9. Fish J, Duerst R, Gelfand E, et al. Challenges in the use of allogeneic hematopoietic SCT for ectodermal dysplasia with immune deficiency. Bone Marrow Transplant. 2009;43:217–21.
10. Permaul P, Narla A, Hornick J, et al. Allogeneic hematopoietic stem cell transplantation for X-linked ectodermal dysplasia and immunodeficiency: case report and review of outcomes. Immunol Res. 2009;44:89–98.
11. Cheng L, Kanwar B, Tcheurekdjian H, et al. Persistent systemic inflammation and atypical enterocolitis in patients with NEMO syndrome. Clin Immunol. 2009;132:124–31.
12. Hanson E, Monaco-Shawver L, Solt L, et al. Hypomorphic nuclear factor-kappaB essential modulator mutation database and reconstitution system identifies phenotypic and immunologic diversity. J Allergy Clin Immunol. 2008;122:1169–1177.e1116.
13. Takada H, Nomura A, Ishimura M, et al. NEMO mutation as a cause of familial occurrence of Behçet's disease in female patients. Clin Genet. 2010;78:575–9.
14. Marks DJ, Miyagi K, Rahman FZ, et al. Inflammatory bowel disease in CGD reproduces the clinicopathological features of Crohn's disease. Am J Gastroenterol. 2009;104:117–24.
15. Nenci A, Becker C, Wullaert A, et al. Epithelial NEMO links innate immunity to chronic intestinal inflammation. Nature. 2007;446:557–61.
16. Nagano M, Kimura N, Ishii E, et al. Clonal expansion of alphabeta-T lymphocytes with inverted Jbeta1 bias in familial hemophagocytic lymphohistiocytosis. Blood. 1999;94:2374–82.
17. Kimura N, Toyonaga B, Yoshikai Y, et al. Sequences and repertoire of the human T cell receptor alpha and beta chain variable region genes in thymocytes. Eur J Immunol. 1987;17:375–83.
18. Nishikomori R, Akutagawa H, Maruyama K, et al. X-linked ectodermal dysplasia and immunodeficiency caused by reversion mosaicism of NEMO reveals a critical role for NEMO in human T-cell development and/or survival. Blood. 2004;103:4565–72.
19. Ogura Y, Imamura Y, Murakami Y, et al. Intracellular cytokine patterns of peripheral blood T cells as a useful indicator of activeness of Crohn's disease. Hiroshima J Med Sci. 2005;54:1–8.
20. Stephan V, Wahn V, Le Deist F, et al. Atypical X-linked severe combined immunodeficiency due to possible spontaneous reversion of the genetic defect in T cells. N Engl J Med. 1996;335:1563–7.
21. Wada T, Yasui M, Toma T, et al. Detection of T lymphocytes with a second-site mutation in skin lesions of atypical X-linked severe combined immunodeficiency mimicking Omenn syndrome. Blood. 2008;112:1872–5.
22. Hirschhorn R, Yang D, Puck J, et al. Spontaneous in vivo reversion to normal of an inherited mutation in a patient with adenosine deaminase deficiency. Nat Genet. 1996;13:290–5.
23. Wada T, Toma T, Okamoto H, et al. Oligoclonal expansion of T lymphocytes with multiple second-site mutations leads to

Omenn syndrome in a patient with RAG1-deficient severe combined immunodeficiency. Blood. 2005;106:2099–101.
24. Ariga T, Kondoh T, Yamaguchi K, et al. Spontaneous in vivo reversion of an inherited mutation in the Wiskott–Aldrich syndrome. J Immunol. 2001;166:5245–9.
25. Filipe-Santos O, Bustamante J, Haverkamp MH, et al. X-linked susceptibility to mycobacteria is caused by mutations in NEMO impairing CD40-dependent IL-12 production. J Exp Med. 2006;203:1745–59.
26. Nenci A, Huth M, Funteh A, et al. Skin lesion development in a mouse model of incontinentia pigmenti is triggered by NEMO deficiency in epidermal keratinocytes and requires TNF signaling. Hum Mol Genet. 2006;15:531–42.
27. Van den Brande J, Braat H, van den Brink G, et al. Infliximab but not etanercept induces apoptosis in lamina propria T-lymphocytes from patients with Crohn's disease. Gastroenterology. 2003;124:1774–85.
28. Nos P, Bastida G, Beltran B, et al. Crohn's disease in common variable immunodeficiency: treatment with antitumor necrosis factor alpha. Am J Gastroenterol. 2006;101:2165–6.
29. Chua I, Standish R, Lear S, et al. Anti-tumour necrosis factor-alpha therapy for severe enteropathy in patients with common variable immunodeficiency (CVID). Clin Exp Immunol. 2007;150:306–11.
30. Uzel G, Orange JS, Poliak N, et al. Complications of tumor necrosis factor-α blockade in chronic granulomatous disease-related colitis. Clin Infect Dis. 2010;51:1429–34.
31. Mackey AC, Green L, Liang LC, et al. Hepatosplenic T cell lymphoma associated with infliximab use in young patients treated for inflammatory bowel disease. J Pediatr Gastroenterol Nutr. 2007;44:265–7.
32. Mackey AC, Green L, Leptak C, et al. Hepatosplenic T cell lymphoma associated with infliximab use in young patients treated for inflammatory bowel disease: update. J Pediatr Gastroenterol Nutr. 2009;48:386–8.
33. Diak P, Siegel J, La Grenade L, et al. Tumor necrosis factor alpha blockers and malignancy in children: forty-eight cases reported to the Food and Drug Administration. Arthritis Rheum. 2010;62:2517–24.

J Clin Immunol (2011) 31:802–810
DOI 10.1007/s10875-011-9568-9

Disseminated BCG Infection Mimicking Metastatic Nasopharyngeal Carcinoma in an Immunodeficient Child with a Novel Hypomorphic *NEMO* Mutation

Masaru Imamura · Tomoki Kawai · Satoshi Okada · Kazushi Izawa · Takayuki Takachi · Haruko Iwabuchi · Sakiko Yoshida · Ryosuke Hosokai · Hirokazu Kanegane · Tatsuo Yamamoto · Hajime Umezu · Ryuta Nishikomori · Toshio Heike · Makoto Uchiyama · Chihaya Imai

Received: 25 February 2011 / Accepted: 3 July 2011 / Published online: 14 July 2011

Abstract
Background Nuclear factor-κB essential modulator (NEMO) deficiency is a developmental and immunological disorder. The genetic and phenotypic correlation has been described.
Methods We report a unique clinical presentation and the identification of a novel missense mutation in the *NEMO* gene in a 3-year-old boy with bacillus Calmette-Guerin (BCG) infection.
Results The patient presented with fever, cervical lymphadenopathy, and abnormal anti-Epstein–Barr virus (EBV) antibody titers, suggestive of EBV-related diseases including chronic active EBV infection, X-linked lymphoproliferative syndrome, or nasopharyngeal carcinoma. Although the biopsy specimen from a nasopharyngeal lesion was initially diagnosed as squamous cell carcinoma, this was changed to disseminated BCG infection involving the nasopharynx, multiple systemic lymph nodes, and brain. A novel mutation (designated D311E) in the *NEMO* gene, located in the NEMO ubiquitin-binding (NUB) domain, was identified as the underlying cause of the immunodeficiency. Impaired immune responses which are characteristic of patients with NEMO deficiency were demonstrated. The patient underwent successful unrelated bone marrow transplantation at 4.9 years of age.
Conclusion This study suggests the importance of the NUB domain in host defense against mycobacteria. The unique presenting features in our patient indicate that a hypomorphic *NEMO* mutation can be associated with atypical

M. Imamura · T. Takachi · H. Iwabuchi · S. Yoshida · R. Hosokai · M. Uchiyama · C. Imai (✉)
Division of Pediatrics, Department of Homeostatic Regulation and Development, Niigata University Graduate School of Medical and Dental Sciences,
1-757 Asahimachi-Dori, Chuo-ku,
Niigata 951-8510, Japan
e-mail: chihaya@med.niigata-u.ac.jp

T. Kawai · K. Izawa · R. Nishikomori · T. Heike
Department of Pediatrics,
Kyoto University Graduate School of Medicine,
Kyoto, Japan

S. Okada
Department of Pediatrics,
Hiroshima University Graduate School of Biomedical Sciences,
Hiroshima, Japan

H. Kanegane
Department of Pediatrics, Graduate School of Medicine,
University of Toyama,
Toyama, Japan

T. Yamamoto
Division of Bacteriology, Department of Infectious Disease Control and International Medicine, Niigata University Graduate School of Medical and Dental Sciences,
Niigata, Japan

H. Umezu
Division of Cellular and Molecular Pathology,
Department of Cellular Function, Niigata University Graduate School of Medical and Dental Sciences,
Niigata, Japan

pathological findings of the epithelial tissues in patients with BCG infection.

Keywords Nuclear factor-κB essential modulator · immunodeficiency · bacillus Calmette-Guerin · squamous cell carcinoma · hematopoietic stem cell transplantation

Introduction

Nuclear factor-κB essential modulator (NEMO) is a 419-amino acid regulatory protein encoded by 10 exons on the X-chromosome [1]. NF-κB is restrained in the cytoplasm by its inhibitor, IκB. NEMO participates in the IκB kinase (IKK) complex, which also contains the IKKα and IKKβ kinases. The IKK complex enables the ubiquitination and degradation of IκB, allowing translocation of NF-κB dimers to the nucleus where gene transcription occurs [2].

X-linked recessive ectodermal dysplasia with immunodeficiency (EDA-ID) is a developmental and immunologic disorder caused by hypomorphic *NEMO* mutations. Ectodermal dysplasia presents with aberrant development of hair (hypotrichosis or atrichosis), teeth (hypodontia, or anodontia with conical incisors), and eccrine sweat glands (hypohidrosis or anhidrosis) [3–5]. NEMO deficiency impairs B cell function, T cell development and survival, natural killer cell cytotoxicity, and toll-like receptor-mediated immune responses [6]. The immunological characteristics of NEMO deficiency include abnormal immunoglobulin production (e.g., hypogammaglobulinemia, hyper IgA, hyper IgM) and specific antibody deficiencies. Various hypomorphic mutations have been found and their association with clinical and immunologic phenotypes has been described [6, 7]. Hypomorphic *NEMO* mutations are associated with ectodermal dysplasia in 77% of patients, serious pyogenic infection in 86%, mycobacterial infection in 39%, serious viral infection in 19%, and inflammatory diseases in 23% [7].

Here, we present a patient with NEMO deficiency caused by a novel mutation. The patient presented with disseminated bacillus Calmette-Guerin (BCG) infection involving the nasopharynx and was initially misdiagnosed with squamous cell carcinoma (SCC).

Patient and Methods

Case Report

The patient (a Japanese boy) was born to nonconsanguineous parents. His maternal uncle died of nontuberculous mycobacterial infection at the age of 18 years. The patient was vaccinated with BCG at 5 months of age without any acute complications. The patient never experienced a serious infection until 30 months of age, when he presented with recurrent fever and cervical lymphadenopathy lasting for 5 months. At 36 months of age, he was referred to Niigata University Medical and Dental Hospital because of abnormal levels of Epstein–Barr virus (EBV) antibodies and a presumed diagnosis of chronic active EBV infection.

His eyebrows, eyelashes, and hair were normal, and there was no facial dysmorphism. His teeth were sparse, with no hypodontia. There was swelling of multiple lymph nodes on the bilateral neck (Fig. 1a), supraclavicular, axillary, and inguinal regions. No abnormal neurological findings were present.

Peripheral blood analysis showed a white blood cell count of 7.0×10^9/l with 48% polymorphonuclear neutrophils and 45% lymphocytes. Serum immunoglobulin (Ig) levels were as follows: IgG 1,180 mg/dl with normal levels of IgG subclasses, IgA 477 mg/dl, IgM 30 mg/dl, IgE

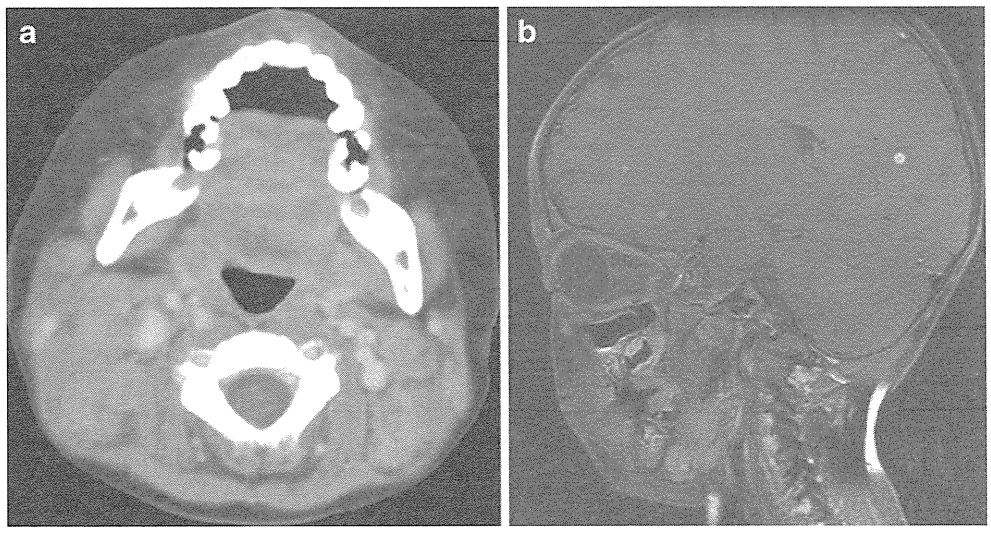

Fig. 1 **a** An axial CT scan with contrast enhancement showing swelling of multiple lymph nodes on the bilateral neck. **b** T1-weighted MRI image. The *arrowheads* indicate multiple contrast-enhanced lesions in the right cerebellar peduncle and subcortical white matter

7.7 IU/ml, and IgD 6.7 mg/dl. Although the patient was given the combined measles–rubella vaccine at 15 months of age, measles IgG was undetectable by enzyme immunoassay (rubella IgG was detected). Titers of anti-EBV antibodies were: EBV viral capsid antigen (VCA) IgG, 1:320; VCA IgA, 1:20; VCA IgM, <1:10; early antigen (EA) IgG, <1:10; EA IgA, <1:10; and EB nuclear antigen, <1:10. Quantitative real-time PCR showed a mildly increased copy number of EBV-DNA (100 copies/μg DNA) in peripheral blood mononuclear cells (PBMCs). Peripheral blood lymphocytes comprised 67% $CD3^+$ T cells, 26% $CD19^+$ B cells, and 1.7% $CD3^-CD56^+$ NK cells. The responses to phytohemagglutinin and concanavalin A were normal. The delayed hypersensitivity test for the purified protein derivative was negative. NK cell activity was 17% (healthy controls, 18–40%). Normal expression of SLAM-associated protein was demonstrated by flow cytometry [8].

Because of the elevated EBVCA-IgA titers, we performed flexible nasopharyngoscopy to rule out nasopharyngeal carcinoma and identified whitish lesions on the posterior nasopharyngeal wall. Surprisingly, frozen sections from the biopsy specimen showed epithelial thickening with loss of the architectural orientation, atypical epithelial cells harboring enlarged nuclei with prominent nucleoli, single cell keratinization, and increased mitotic figures, and strongly suggested SCC (Fig. 2a, b). An MRI scan of the brain showed multiple contrast-enhanced lesions in the right cerebellar peduncle and subcortical white matter, suggesting distant metastases (Fig. 1b). Because nasopharyngeal carcinoma in this age group is extremely rare [9], we investigated the presence and monoclonality of the EBV genome in the cryopreserved biopsied tissue by Southern blotting with a terminal-repeat probe, which turned out to be negative. Nine days after the biopsy, a formalin-fixed paraffin-embedded specimen (which had been simultaneously but independently biopsied from the pharyngeal lesion) showed granulomatous lesions with marked inflammatory cell infiltration in the subepithelial layer in addition to atypical squamous epithelium (Fig. 2c). EBV-encoded RNA (EBER)-1 was not detected. A Ziehl–Neelsen stain, performed because macrophage infiltration without caseous necrosis under the epithelium was observed, showed numerous acid-fast bacilli (Fig. 2d). A cryopreserved tissue specimen from the pharyngeal lesion was subjected to an acid-fast bacilli culture and gave a positive result. Thereafter, BCG was identified by PCR. Cultures of peripheral blood and gastric juices for acid-fast bacilli were also positive, but the cerebrospinal fluid was negative. According to these findings, a diagnosis of disseminated BCG infection was made.

The patient was treated with isoniazid and rifampicin along with an 8-week course of pyrazinamide and intramuscular streptomycin, and his symptoms rapidly resolved. Nasopharyngoscopy and biopsy after 1 month of therapy was normal, as were the culture results. Six months later, an MRI scan of the brain showed that the multiple nodules had disappeared. Although the disseminated BCG infection was

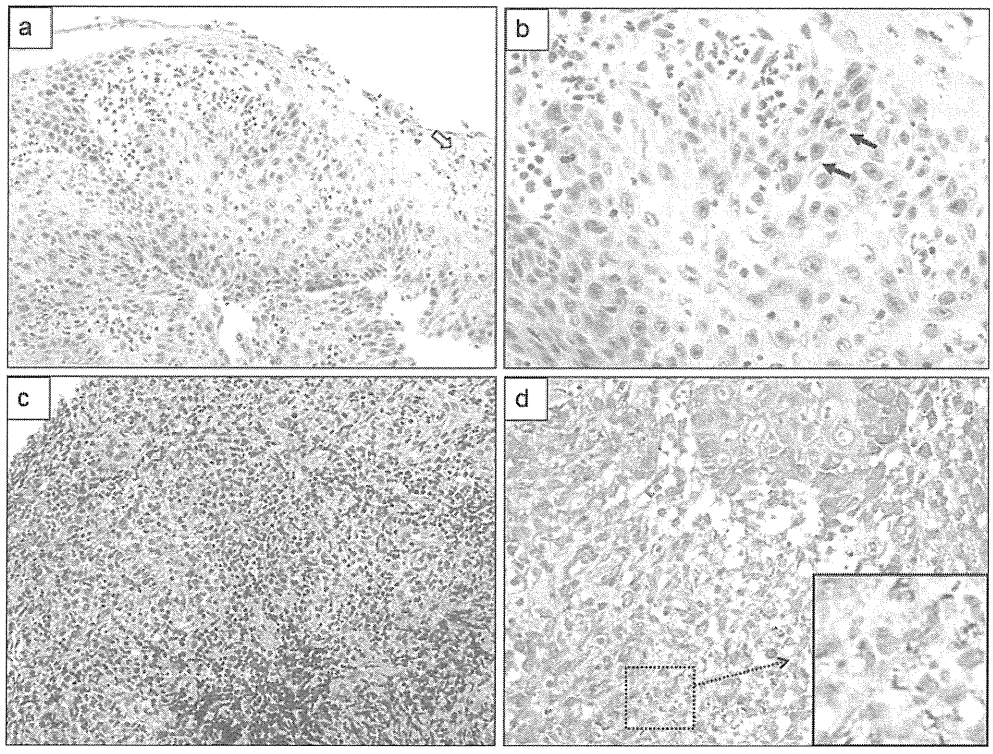

Fig. 2 Biopsy specimens of the posterior nasopharyngeal wall. **a**, **b** The frozen sections showed epithelial thickening with loss of the architectural orientation, atypical epithelial cells harboring enlarged nuclei with prominent nucleoli, single cell keratinization (**a**, *open arrow*), and increased mitotic figures (**b**, *closed arrow*) (hematoxylin and eosin stain, original magnification **a** ×200; **b** ×1,000). **c** In a formalin-fixed paraffin-embedded specimen, granulomatous lesions with marked inflammatory cell infiltration were found in the subepithelial layer (hematoxylin and eosin stain, original magnification ×200). **d** Numerous red-purple materials were scattered in a Ziehl–Neelsen stain, indicating acid-fast bacilli (original magnification ×400)

successfully treated, the patient continued to present with recurrent infections, including cervical lymphadenitis, parotitis, and pneumococcal sepsis.

Flow Cytometric Analysis

After informed consent was obtained, heparinized venous blood was collected from the patient and the normal control according to the approval of the Ethics Committees of Hiroshima University and Kyoto University. PBMCs were prepared by density gradient centrifugation. For NEMO intracellular staining, the cells were fixed, permeabilized, and washed with Permfix and Permwash (BD Biosciences Pharmingen, San Diego, CA, USA), and stained sequentially with a mouse anti-NEMO mAb (1 μg/ml; C73-764 or clone 54; BD Biosciences Pharmingen) and a phycoerythrin-labeled goat anti-mouse IgG Ab (DAKO Japan Co, Kyoto, Japan) as previously described [10]. The cells were stained for the following lineage markers after staining for NEMO: CD3, CD14, CD19, and CD56 (BD Biosciences Pharmingen). For CD40L stimulation, PBMCs were cultured with recombinant soluble human CD40L (rCD40L; 2.5 μg/ml; PeproTech Inc, Rocky Hill, NJ, USA) for 48 h and then stained for CD23, CD54, CD86, CD95, and CD19 (BD Biosciences Pharmingen).

Genetic Analysis

The genetic analysis was performed as previously described [11]. PBMCs were cultured for 4 days in RPMI 1640 with 10% fetal calf serum (HyClone, Thermo Scientific, MA, USA), interleukin-2 (100 ng/ml; R&D systems, Minneapolis, MN, USA), and phorbol myristate acetate (1 μg/ml; Sigma-Aldrich, St. Louis, MO, USA). Total RNA was extracted and complementary DNA (cDNA) was synthesized using random hexamer (Invitrogen, Carlsbad, CA, USA). PCR was performed using the cDNA along with primers that spanned the entire coding region of *IKBKG* (forward, 5′-CCC AAG CTT CCC TTG CCC TGT TGG ATG AAT AGG-3′ and reverse, 5′-CGC GGA TCC AGG TGG CAT CCC ACT TGT GG-3′). The PCR products were sequenced using a BigDye Terminator v3.1 cycle sequencing kit and ABI PRISM 310 genetic analyzer (Applied Biosystems, Foster City, CA, USA), and the primers used were as follows: 5′-ACT GCG CTC TAT CGA GGT C-3′, 5′-TGG AGG AGA ATC AAG AGC TC-3′, 5′-CAG AGT CGC TTG GAG GCT G-3′, 5′-AGG AGG TGA TCG ATA AGC TG-3′, and 5′-CTG CCT CTT CAG ATC GAG C-3′, 5′-CAT CAC AAT CTT GTG CTG CTC GG-3′. Genomic DNA was also extracted from peripheral blood leukocytes. Exon 8 of *IKBKG* and its flanking intron were amplified using the following primers: 5′-ACT TGT GCT GCT CCT TAG AC-3′ and 5′-ATG CCG CTT CCT CAT GTC C-3′, and sequenced.

Cytokine Release Assay

PBMCs were stimulated with varying doses of IL-18 with IL-12 (20 ng/ml; R&D Systems Inc) or varying doses of lipopolysaccharide (LPS; Sigma) with or without interferon-γ (IFN-γ; 5,000 U/ml; R&D Systems Inc). Forty-eight hours later, the supernatant was harvested, and the cytokines were measured using human BD OptEIA enzyme-linked immunosorbent assay kits (BD Biosciences Pharmingen) as previously described [10].

Immunohistochemical Analysis of NEMO Expression

Formalin-fixed paraffin-embedded specimens from the pharyngeal lesions of the patient were stained with a rabbit anti-NEMO polyclonal antibody (FL-419, Santa Cruz Biotechnology, Santa Cruz, CA, USA) with standard techniques. Specimens from the pharyngeal lesion of an adolescent female patient with EBV-positive nasopharyngeal SCC served as control.

Plasmids, Transfection, and Western Blotting

The cDNA of the wild-type and mutant NEMO (NEMO-D311E) were generated from PBMCs of a healthy volunteer and the patient by reverse transcription-PCR, respectively. The cDNA was subcloned into p3xFLAG-CMV14 vector (Sigma). The NEMO-null rat fibroblast cells (kindly provided by S. Yamaoka) were transfected with a plasmid encoding the wild-type or mutant NEMO, or the corresponding mock vector, by using FuGENE® HD Transfection Reagent (TOYO-B-Net, Tokyo, Japan) according to the manufacturer's protocol, and were subjected to an immunoblot analysis. Cell lysates were electrophoresed with sodium dodecyl sulfate-polyacrylamide gel electrophoresis (SDS-PAGE), and immunoblotting was performed using a mouse anti-NEMO mAb (C73-764; BD Biosciences Pharmingen) and a horseradish peroxidase-conjugated rabbit anti-mouse IgG polyclonal antibody, as previously described [10]. The same blots were reprobed with anti-FLAG mAb (clone M2, Sigma-Aldrich) or a mouse anti-β-actin mAb (ACTBD11B7; Santa Cruz Biotechnology).

Results

Identification of a Novel Missense Germline Mutation in *NEMO*

NEMO expression was not detected in the patient's $CD3^+$, $CD19^+$, $CD14^+$, and $CD56^+$ cells by flow cytometry using anti-NEMO mAb (Fig. 3a). Interestingly, normal NEMO expression was observed in a small proportion of $CD3^+$ T

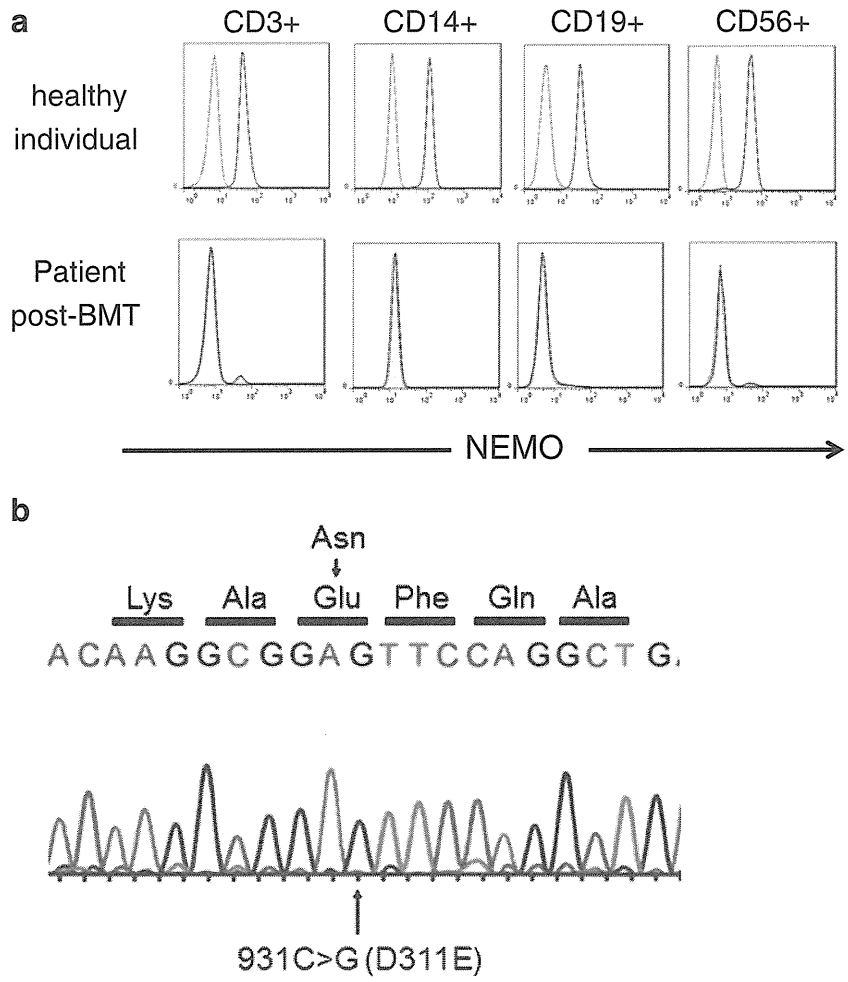

Fig. 3 Identification of a novel hypomorphic NEMO mutation. **a** The intracellular staining of NEMO protein was performed using anti-NEMO mAb. NEMO expression was not detected in all immune cell lineages studied. *Open areas* indicate anti-NEMO mAbs and *closed areas* indicate the isotype controls. **b** A novel missense mutation (931 C>G, designated D311E) in the *NEMO* gene was identified by cDNA analysis. The mutation was confirmed by analysis of genomic DNA from the patient's peripheral blood leukocytes

cells. Subsequently, a novel missense mutation in the *NEMO* gene (931 C>G, designated D311E) was identified by cDNA analysis (Fig. 3b). The mutation was confirmed by analysis of genomic DNA from the patient's peripheral blood leukocytes. His mother was also found to be heterozygous for this mutation. No mutations in the *NEMO* gene were detected in the patient's healthy brother or father.

To clarify the functional defects, we investigated B cell responses to rhsCD40L using flow cytometry. The results showed that up-regulation of CD23, CD54, CD86, and CD95 by $CD19^+$ B cells in response to rhsCD40L was severely impaired (Fig. 4a). In addition, we investigated cytokine release from the patient's PBMCs in response to the stimuli which activate the NF-κB signaling pathway through NEMO (Fig. 4b). In the PBMCs from the patient, IFN-γ secretion induced by treatment with IL-18 and IL-12 was severely impaired. Similarly, TNF-α secretion in response to LPS stimulation in the absence or presence of IFN-γ was severely impaired. Thus, we demonstrated in the present case impaired immune functions typically seen in patients with NEMO deficiency.

Bone Marrow Transplantation

At 4.9 years of age, human leukocyte antigen matched (10 matches out of 10 alleles) unrelated bone marrow transplantation (UBMT) was performed. The preconditioning regimen consisted of fludarabine (30 mg/m^2) on days −7 to −3, melphalan (70 mg/m^2) on days −6 to −5, and rabbit anti-thymocyte globulin (1.25 mg/kg) on days −5 to −2. The patient received 5.9×10^8 nucleated cells/kg (containing 5.8×10^6 $CD34^+$ cells/kg) from a male donor. Tacrolimus (0.02 mg/kg/day), mycophenolate mofetil (MMF, 30 mg/kg/day b.i.d.) and methylprednisolone (2 mg/kg/day) were used for graft-versus-host disease (GVHD) prophylaxis. The conditioning regimen was well tolerated with no severe complications. Neutrophil engraftment (neutrophils>0.5×10^9/l) and platelet engraftment (50×10^9 platelets/l) were documented on days +10 and +15, respectively, with complete donor chimerism. Although grade I acute GVHD (skin) occurred on day +46, it resolved without the need for corticosteroid therapy. The only infectious complication was asymptomatic CMV antigenemia. Twenty months after receiving UBMT, the patient enjoys a normal life without

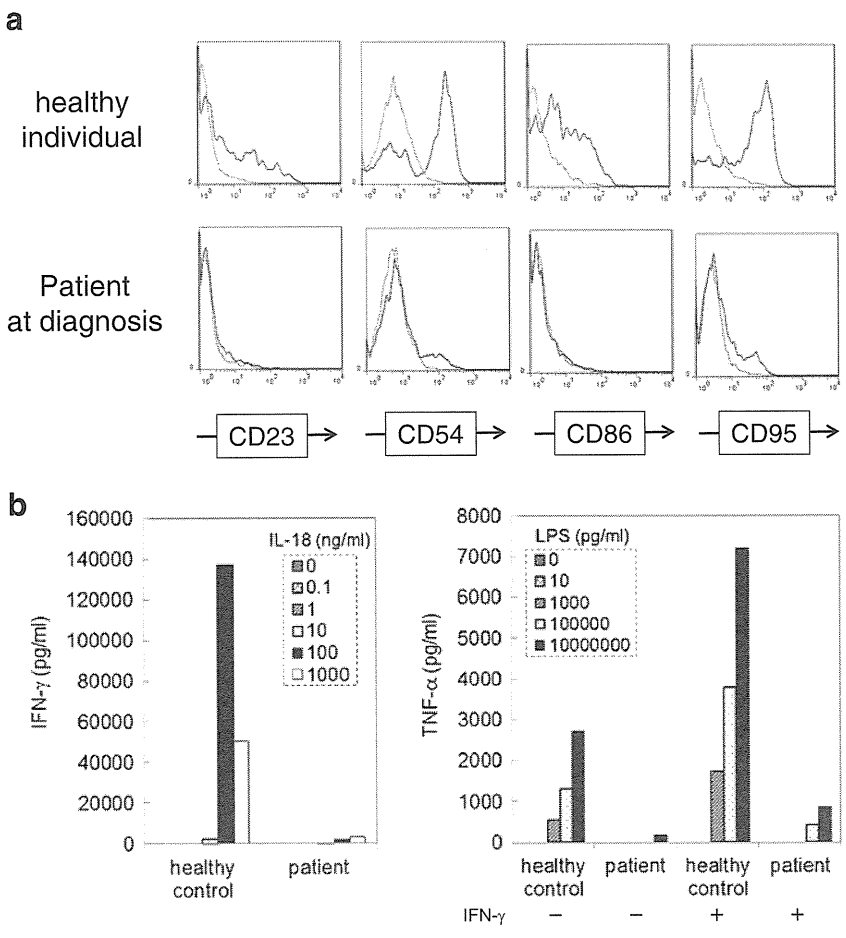

Fig. 4 Functional analysis of immune cells. **a** Induction of CD23, CD54, CD86, and CD95 in response to rhsCD40L stimulation was severely reduced in the patient's B cells. *Open areas* indicate the indicated mAbs and *closed areas* indicate the isotype controls. **b** PBMCs from the patient and healthy controls were stimulated with varying doses of IL-18 plus IL-12 (20 ng/ml) or with varying doses of LPS with or without IFN-γ (5,000 U/ml). Cytokine release from the patient's PBMCs in response to the stimuli which activate the NF-κB signaling pathway through NEMO was severely impaired

any signs of either chronic GVHD or gastrointestinal symptoms, except for the occurrence of multiple papillomas on the foot soles and fingers. After successful UBMT, NEMO protein expression and in vitro $CD19^+$ B cell responses to rhsCD40L were completely restored (Fig. 5a, b).

Protein Expression of D311E Mutant

In the present case, NEMO protein was not detected in all immune cell lineages by flow cytometry using anti-NEMO mAb, while we demonstrated impaired immune responses typically seen in patients with NEMO deficiency. These observations confirmed a diagnosis of congenital NEMO deficiency with immunodeficiency. However, we felt that it might be difficult to reconcile the benign infectious disease history of the first 30 months of life and very mild EDA features (teeth which seem to be apparently sparse in comparison to those of his 1-year-older brother who does not carry mutant *NEMO*) with a near total absence of NEMO in immune cells. Therefore, we sought to examine whether D311E mutation in the *NEMO* gene can really result in defect of the NEMO protein. For this purpose, we analyzed NEMO protein expression in the patient's tissue immunohistochemically. We observed the presence of NEMO protein by using polyclonal anti-NEMO antibody in the patient's biopsy specimens from the pharyngeal epithelial tissue before and after the successful anti-mycobacterial treatment, although anti-NEMO mAb did not give a positive staining (data not shown). In addition, we further analyzed expression of mutant NEMO protein by Western blotting. Because the patient's own PBMCs were no longer available at that time, we transfected NEMO-null rat fibroblast cells with a plasmid encoding *NEMO* carrying D311E mutation and analyzed NEMO protein expression by Western blotting. As observed in flow cytometry, NEMO protein was not detected in cells transfected with *NEMO*-D311E mutant by using the same monoclonal antibody. However, FLAG-tagged protein was demonstrated by anti-FLAG mAb, indicating the presence of NEMO protein (Fig. 6). The amount of FLAG-tagged protein was comparable to that in cells transfected with a wild-type *NEMO* cDNA. These findings strongly suggested that mutant protein is expressed by the mutated *NEMO* gene carrying D311E and is present in the patient's tissue.

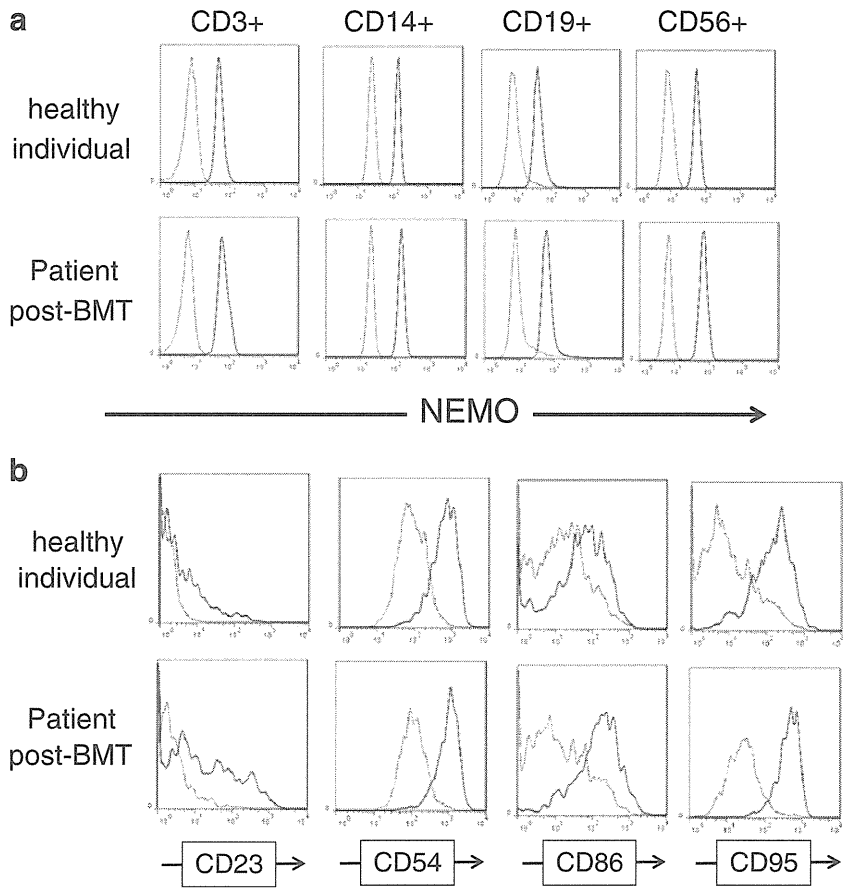

Fig. 5 Restoration of NEMO expression and function after BMT. **a** Intracellular NEMO expression was detected in all immune cell lineages after successful BMT. **b** Expression of CD23, CD54, CD86, and CD95 on $CD19^+$ B cells induced by rhsCD40L stimulation was comparable to those observed in a healthy subject, indicating restoration of functional properties of immune cells after BMT. *Open areas* indicate the indicated mAbs and *closed areas* indicate the isotype controls

Discussion

In the present study, we identified a novel missense mutation, D311E, in the NEMO ubiquitin-binding (NUB) domain of the *NEMO* gene in a patient with EDA-ID. The patient presented with disseminated BCG infection which mimicked metastatic SCC. NEMO protein was not detected in the patient's immune cells by using anti-NEMO mAb, but in vitro experiments revealed that the NEMO protein is produced by the mutant *NEMO* gene. These observations suggested that the epitope recognized by the anti-NEMO mAb used in this study is altered and its antigenicity is changed. The presence of mutant NEMO protein in the tissue suggests that the mutant NEMO protein mostly allowed signaling which is required for the development of the ectodermal tissues but caused immune dysfunction and abnormal epithelial differentiation in response to severe BCG infection.

Two other EDA-ID-causing mutations within the same amino acid, D311N and D311G, have been identified, and these mutations do not impair NEMO protein production and folding [12, 13]. These two mutations impair the K63-linked and linear polyubiquitin binding functions of NEMO, resulting in impaired NF-κB activation. We expect that a similar mechanism may be operated in NEMO-D311E, but an exact role of K63-linked ubiquitination in this novel mutant remains to be determined in future experiments. Both aspartic acid (wild type) and glutamic acid (in the present patient) are acidic amino acids, whereas asparagine and glycine are uncharged polar and non-polar neutral amino acids, respectively. Thus, we may assume that the D311E substitution is less deleterious than the D311G and D311N mutations. In line with this, the D311E mutation caused a milder EDA phenotype, in comparison with the D311G and D311N, which were reported to cause more apparent features of EDA including dental agenesis and abnormal dentition with spike-like lower teeth. In the present patient, EDA symptoms included only very mild dental abnormalities (sparse teeth). In general, patients with immunodeficiency have an increased risk of developing severe systemic tuberculosis or disseminated BCG infection [14, 15]. Indeed, nearly 40% of patients with hypomorphic NEMO mutations suffer from mycobacterial infections [7]. The high susceptibility to mycobacterial infections observed in patients with mutations in the NUB domain, including D311N, D311G, E315A, R319Q [12, 13, 16], and D311E, suggest the importance of this domain in host defense against mycobacteria.

The pathologic findings for BCG infection in immunocompetent and immunocompromised patients can be

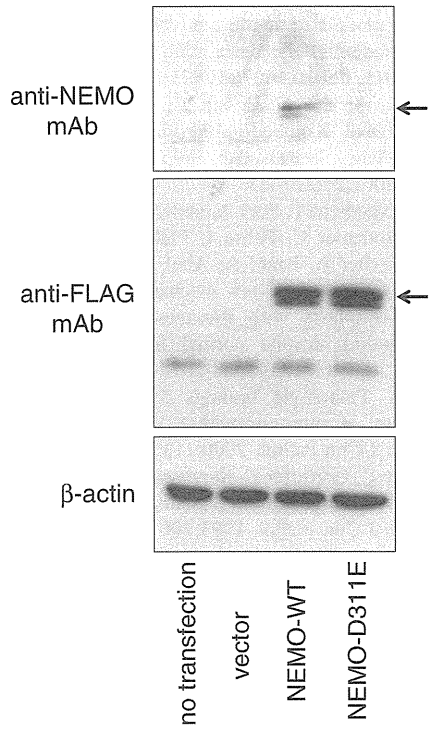

Fig. 6 In vitro expression of NEMO-D311E. The NEMO-null rat fibroblast cells were transfected with a plasmid encoding the wild-type or mutant NEMO, or the corresponding mock vector. Cell lysates were electrophoresed with SDS-PAGE and immunoblotted with a mouse anti-NEMO mAb (C73-764) or anti-FLAG mAb (clone M2). β-Actin was used as a control for equal loading. Anti-NEMO mAb only detected wild-type NEMO protein. By contrast, FLAG-tagged protein was demonstrated by anti-FLAG mAb in both transfectants with wild-type *NEMO* and *NEMO*-D311E, indicating the presence of NEMO protein at quantitatively normal levels

different [14, 15]. The former show multiple epithelioid granulomas, Langhans giant cells with, or without, suppuration, minimal caseous necrosis, and scanty acid-fast-positive organisms. The latter show poorly formed granulomas, proliferation of sheets of plump oval or spindle-shaped histiocytic cells, variable necrosis, and abundant acid-fast-positive organisms. In some immunocompromised patients with BCG infection, biopsy specimens resemble Langerhans cell histiocytosis, fibrohistiocytic neoplasm, or pseudotumors [14, 17]. In the present case, the nasopharyngeal involvement of the disseminated BCG infection clinically and pathologically mimicked SCC. It is interesting to speculate that NEMO deficiency in the epithelial cells may also have played a role in the formation of the SCC-like lesions. Expression of IKKα, one of the components of the IKK complex, is markedly reduced in poorly differentiated human and mouse skin SCC [18]. Furthermore, *IKKα* mutations were found in 8/9 human SCCs [18]. In animal experiments, $IKK\alpha^{+/-}$ mice are more susceptible to chemical carcinogen-induced squamous cell carcinoma and papillomas than $IKK\alpha^{+/+}$ mice [19]. These observations suggest that NF-κB signaling is one of the key regulators of epithelial cell transformation. Although direct evidence showing that NEMO deficiency, or mutation, involved in human carcinogenesis is lacking, dysregulation of NF-κB signaling in association with BCG infection may have induced the formation of pseudocarcinomatous epithelium in the present patient.

Nasopharyngeal involvement of tuberculosis can be primary or secondary to other sites of infection, especially to pulmonary disease, and nasopharyngeal involvement occurs in only 0.1% of patients with active pulmonary tuberculosis [20]. To the best of our knowledge, nasopharyngeal BCG infection has not been reported previously.

The long-term prognosis for patients with NEMO deficiency is poor. In one study, one third of NEMO-deficient patients died at a mean age of 6.4 years unless the immunological disorders were corrected [7]. Our case is the first NEMO-deficient patient to be successfully treated with an unrelated BMT after a reduced intensity conditioning regimen. Because methotrexate (MTX) can cause severe liver toxicity in patients with a *NEMO* mutation [21], we used MMF and corticosteroids instead of MTX for GVHD prophylaxis. The treatment course of hematopoietic stem cell transplantation (HSCT) was excellent. Although HSCT is currently the only treatment for correcting immunodeficiency, few successful cases have been reported in patients with NEMO deficiency [21–24]. Factors which may contribute to the outcome of HSCT for NEMO deficiency is still unclear due to a small number of HSCT cases reported and high diversity in the conditioning regimens, the stem cell source, and GVHD prophylaxis. Interestingly, among the four cases who survived HSCT, three patients harbored the same mutation, 1167-1168insC [24]. To see a phenotype/genotype correlation in HSCT outcome for NEMO deficiency, further accumulation of patients who undergo HSCT is needed.

In conclusion, we have presented a patient with EDA-ID caused by a novel hypomorphic *NEMO* mutation. A hypomorphic *NEMO* mutation in a patient with BCG infection may be associated with atypical pathological features mimicking SCC. Dysfunctional NEMO protein in nonhematopoietic cells, such as epithelial cells, is still present, even after successful HSCT. Because of the prolonged survival times that result from successful HSCT and the associated accumulation of environmental genotoxic insults, a higher incidence of SCC in such patients at a relatively young age may become a problem. As the long-term prognosis after HSCT is still unclear, we need to carefully monitor both the general complications that accompany HSCT and other complications caused by surviving NEMO dysfunctional cells. Further pathological and molecular investigation of patients with hypomorphic *NEMO* mutations is required.

Acknowledgments We thank Prof. Jean-Laurent Casanova (The Rockefeller University) for his critical discussion. We also acknowledge Dr. Jacinta Bustamante and Ms. Marjorie Hubeau (Institut National de la Santé et de la Recherche Médicale) for providing D311 mutant *NEMO* plasmids. This study was supported in part by a Grant-in-Aid for Scientific Research from the Ministry of Education, Culture, Sports, Science and Technology of Japan.

Competing Interests None.

References

1. Aradhya S, Bardaro T, Galgóczy P, Yamagata T, Esposito T, Patlan H, et al. Multiple pathogenic and benign genomic rearrangements occur at a 35 kb duplication involving the NEMO and LAGE2 genes. Hum Mol Genet. 2001;10:2557–67.
2. Gilmore TD. Introduction to NF-kappaB: players, pathways, perspectives. Oncogene. 2006;25:6680–4.
3. Ku CL, Dupuis-Girod S, Dittrich AM, Bustamante J, Santos OF, Schulze I, et al. NEMO mutations in 2 unrelated boys with severe infections and conical teeth. Pediatrics. 2005;115:615–9.
4. Niehues T, Reichenbach J, Neubert J, Gudowius S, Puel A, Horneff G, et al. Nuclear factor kappaB essential modulator-deficient child with immunodeficiency yet without anhidrotic ectodermal dysplasia. J Allergy Clin Immunol. 2004;114:1456–62.
5. Orange JS, Levy O, Brodeur SR, Krzewski K, Roy RM, Niemela JE, et al. Human nuclear factor kappa B essential modulator mutation can result in immunodeficiency without ectodermal dysplasia. J Allergy Clin Immunol. 2004;114:650–6.
6. Orange JS, Jain A, Ballas ZK, Schneider LC, Geha RS, Bonilla FA. The presentation and natural history of immunodeficiency caused by nuclear factor kappaB essential modulator mutation. J Allergy Clin Immunol. 2004;113:725–33.
7. Hanson EP, Monaco-Shawver L, Solt LA, Madge LA, Banerjee PP, May MJ, et al. Hypomorphic nuclear factor-kappaB essential modulator mutation database and reconstitution system identifies phenotypic and immunologic diversity. J Allergy Clin Immunol. 2008;122:1169–77.
8. Zhao M, Kanegane H, Kobayashi C, Nakazawa Y, Ishii E, Kasai M, et al. Early and rapid detection of X-linked lymphoproliferative syndrome with SH2D1A mutations by flow cytometry. Cytometry B Clin Cytom. 2011;80:8–13.
9. Sengupta S, Pal R, Saha S, Bera SP, Pal I, Tuli IP. Spectrum of head and neck cancer in children. J Indian Assoc Pediatr Surg. 2009;14(4):200–3.
10. Nishikomori R, Akutagawa H, Maruyama K, Nakata-Hizume M, Ohmori K, Mizuno K, et al. X-linked ectodermal dysplasia and immunodeficiency caused by reversion mosaicism of NEMO reveals a critical role for NEMO in human T-cell development and/or survival. Blood. 2004;103:4565–72.
11. Karakawa S, Okada S, Tsumura M, Mizoguchi Y, Ohno N, Yasunaga S, Ohtsubo M, Kawai T, Nishikomori R, Sakaguchi T, Takihara Y, Kobayashi M. Decreased expression in nuclear factor-κB essential modulator due to a novel splice-site mutation causes X-linked ectodermal dysplasia with immunodeficiency. J Clin Immunol. 2011. doi:10.1007/s10875-011-9560-4
12. Döffinger R, Smahi A, Bessia C, Geissmann F, Feinberg J, Durandy A, et al. X-linked anhidrotic ectodermal dysplasia with immunodeficiency is caused by impaired NF-kappaB signaling. Nat Genet. 2001;27:277–85.
13. Hubeau M, Ngadjeua F, Puel A, Israel L, Feinberg J, Chrabieh M, Belani K, Bodemer C, Fabre I, Plebani A, Boisson-Dupuis S, Picard C, Fischer A, Israel A, Abel L, Veron M, Casanova JL, Agou F, Bustamante J. A new mechanism of X-linked anhidrotic ectodermal dysplasia with immunodeficiency: impairment of ubiquitin binding despite normal folding of NEMO protein. Blood. 2011. doi:10.1182/blood-2010-10-315234
14. al-Bhlal LA. Pathologic findings for Bacille Calmette-Guérin infections in immunocompetent and immunocompromised patients. Am J Clin Pathol. 2000;113:703–8.
15. Abramowsky C, Gonzalez B, Sorensen RU. Disseminated bacillus Calmette-Guérin infections in patients with primary immunodeficiencies. Am J Clin Pathol. 1993;100:52–6.
16. Filipe-Santos O, Bustamante J, Haverkamp MH, Vinolo E, Ku CL, Puel A, et al. X-linked susceptibility to mycobacteria is caused by mutations in NEMO impairing CD40-dependent IL-12 production. J Exp Med. 2006;203:1745–59.
17. Edgar JD, Smyth AE, Pritchard J, Lammas D, Jouanguy E, Hague R, et al. Interferon-gamma receptor deficiency mimicking Langerhans' cell histiocytosis. J Pediatr. 2001;139:600–3.
18. Liu B, Park E, Zhu F, Bustos T, Liu J, Shen J, et al. A critical role for I kappaB kinase alpha in the development of human and mouse squamous cell carcinomas. Proc Natl Acad Sci USA. 2006;103:17202–7.
19. Park E, Zhu F, Liu B, Xia X, Shen J, Bustos T, et al. Reduction in IkappaB kinase alpha expression promotes the development of skin papillomas and carcinomas. Cancer Res. 2007;67:9158–68.
20. Güven Güvenç M, Tuna Edizer D, Altu T, Midilli K, Aygün G. Nasopharyngeal tuberculosis. Rev Laryngol Otol Rhinol. 2007;128:89–91.
21. Tono C, Takahashi Y, Terui K, Sasaki S, Kamio T, Tandai S, et al. Correction of immunodeficiency associated with NEMO mutation by umbilical cord blood transplantation using a reduced-intensity conditioning regimen. Bone Marrow Transplant. 2007;39:801–4.
22. Fish JD, Duerst RE, Gelfand EW, Orange JS, Bunin N. Challenges in the use of allogeneic hematopoietic SCT for ectodermal dysplasia with immune deficiency. Bone Marrow Transplant. 2009;43:217–21.
23. Pai SY, Levy O, Jabara HH, Glickman JN, Stoler-Barak L, Sachs J, et al. Allogeneic transplantation successfully corrects immune defects, but not susceptibility to colitis, in a patient with nuclear factor-kB essential modulator deficiency. J Allegy Clin Immunol. 2008;122:1113–8.
24. Permaul P, Narla A, Hornick JL, Pai SY. Allogeneic hematopoietic stem cell transplantation for X-linked ectodermal dysplasia and immunodeficiency: case report and review of outcomes. Immunol Res. 2009;44:89–98.

J Clin Immunol (2011) 31:946–951
DOI 10.1007/s10875-011-9583-x

Association of *IRF5* Polymorphisms with Susceptibility to Hemophagocytic Lymphohistiocytosis in Children

Masakatsu Yanagimachi · Hiroaki Goto · Takako Miyamae · Keisuke Kadota · Tomoyuki Imagawa · Masaaki Mori · Hidenori Sato · Ryu Yanagisawa · Tetsuji Kaneko · Satoshi Morita · Eiichi Ishii · Shumpei Yokota

Received: 2 May 2011 / Accepted: 9 August 2011 / Published online: 4 September 2011

Abstract
Introduction Hemophagocytic lymphohistiocytosis (HLH) is a hyperinflammatory syndrome and has a varied genetic background. The polymorphism of *interferon regulatory factor 5* gene (*IRF5*) was reported to be associated with susceptibility to macrophage activation syndrome. IRF5 acts as a master transcription factor in the activation of pro-inflammatory cytokines. We assessed associations of *IRF5* gene polymorphisms with susceptibility to secondary HLH.
Methods Three *IRF5* single nucleotide polymorphisms (rs729302, rs2004640, and rs2280714) were genotyped using TaqMan assays in 82 secondary HLH patients and 188 control subjects.
Results There was a significant association of the GT/TT genotype at rs2004640 with secondary HLH susceptibility ($p<0.01$). The *IRF5* haplotype (rs729302 A, rs2004640 T, and rs2280714 T) was associated with secondary HLH susceptibility ($p<0.01$).
Conclusions These findings indicate that *IRF5* is a genetic factor influencing the susceptibility to secondary HLH and that the IRF5-associated immune response contributes to the pathogenesis of HLH.

Keywords Interferon regulatory factor 5 · polymorphisms · hemophagocytic lymphohistiocytosis

Electronic supplementary material The online version of this article (doi:10.1007/s10875-011-9583-x) contains supplementary material, which is available to authorized users.

M. Yanagimachi · H. Goto (✉) · T. Miyamae · K. Kadota · T. Imagawa · M. Mori · S. Yokota
Department of Pediatrics,
Yokohama City University Graduate School of Medicine,
Yokohama, Japan
e-mail: hgoto39@med.yokohama-cu.ac.jp

H. Sato
CNV Laboratory, DNA Chip Research Institute,
Yokohama, Japan

R. Yanagisawa
Department of Pediatrics, Shinshu University School of Medicine,
Matsumoto, Japan

T. Kaneko · S. Morita
Department of Biostatistics and Epidemiology,
Yokohama City University Graduate School of Medicine,
Yokohama, Japan

E. Ishii
Department of Pediatrics,
Ehime University Graduate School of Medicine,
Ehime, Japan

E. Ishii
The HLH Study Committee,
Japanese Pediatric Leukemia/Lymphoma Study Group,
Nagoya, Japan

Introduction

Hemophagocytic lymphohistiocytosis (HLH) is a hyperinflammatory syndrome that is accompanied by serious morbidity [1, 2]. The incidence of HLH is estimated to be about 1.2 cases per million individuals per year [3]. HLH is characterized by prolonged fever, cytopenias, hepatosplenomegaly, and hemophagocytosis in reticuloendothelial systems. The characteristic laboratory findings include hypertriglyceridemia, hyperferritinemia, hypofibrinogeneima, and increased soluble CD25 [1–4]. These manifestations and laboratory values are described as the result of hypercytokinemia caused by an

ineffective immunological response mediated by histiocytes (macrophages and dendritic cells), natural killer (NK) cells, and cytotoxic T cells (CTL) [1, 5–7]. Increased levels of several pro-inflammatory cytokines, such as interleukin-6 (IL-6), interferon (IFN)-γ, and tumor necrosis factor (TNF)-α have been demonstrated in patients with HLH [8–10]. HLH is classified into primary (genetic) or secondary (acquired) HLH. There are two subtypes of primary HLH, namely, familial HLH (FHL) and other immunodeficiencies such as Chediak–Higashi syndrome, Griscelli syndrome type 2, Hermansky–Pudlak syndrome type 2, and the X-linked lymphoproliferative syndrome [2, 11]. Mutations of *perforin* (*PRF1*), *UNC13D*, *STX11*, and *STXBP2* genes are responsible for 30–70% of FHLH cases [12–16]. It is thought that other unknown genetic defects remain as causes of FHL. Secondary HLH may occur under conditions of severe infections, malignancies, or autoimmune diseases [1, 2]. Many viruses, bacteria, and other infectious agents have been reported to trigger infection-associated HLH (IHLH) [17]. Epstein–Barr virus (EBV) is the most studied virus that trigger IHLH [18]. EBV-associated HLH (EBV-HLH) has a higher prevalence in East Asian countries [18]. Therefore, there may be a genetic variation in susceptibility to EBV-HLH.

Genetic factors other than *PRF1*, *UNC13D*, *STX11*, and *STXBP2* might influence susceptibility even to secondary HLH. Macrophage activation syndrome (MAS) is one form of secondary HLH [1, 2]. MAS occurs in patients with autoimmune diseases, especially with systemic-onset juvenile idiopathic arthritis (systemic JIA) [19, 20]. We recently reported that the *interferon regulatory factor 5* (*IRF5*) gene polymorphism is associated with susceptibility to MAS in systemic JIA patients [21]. IRF5 is a member of the IRF family of transcription factors and is known to have a crucial role in the Toll-like receptor signaling pathway [22, 23]. The activation of the Toll-like receptor is central to innate and adaptive immunity. IRF5 acts as a master transcription factor in the activation of pro-inflammatory cytokine genes especially in the virus-mediated immunological signaling pathway [23]. In *IRF5* knockout mice, a severely impaired induction of IL-6, IL-12, and TNF-α was observed [22].

In the present study, we hypothesized that polymorphisms in the *IRF5* gene may be associated with susceptibility to secondary HLH. We found a close relationship between the *IRF5* gene polymorphism/haplotype and susceptibility to secondary HLH.

Patients and Methods

Study Population

Patients with secondary HLH except for MAS were diagnosed based on the diagnostic criteria used in the HLH-94 Study (for patients who developed HLH before October 2006) and HLH-2004 Study (after October 2006) [4, 24]. The patients who showed known genetic mutations were excluded as primary HLH in this study. Patients under 1 year were also excluded to reduce the possible inclusion of undiagnosed primary HLH because the onset of FHL is below 1 year of age in 70–80% of the cases [25].

Patients with MAS were diagnosed as having systemic JIA based on the International League of Associations for Rheumatology classification criteria for systemic JIA [26]. Because the HLH-94/2004 diagnostic criteria may not always be appropriate when diagnosing MAS in systemic JIA patients who are under inflammatory conditions, patients with systemic JIA were diagnosed as having MAS based on the preliminary diagnostic guidelines for MAS complicating systemic JIA [27], as follows: (1) clinical criteria including central nervous dysfunction, hemorrhage or hepatomegaly and (2) laboratory criteria including decreased platelet counts ($<26.2\times10^9$/l), elevated levels of asparate aminotransferase (>59 U/l), decreased white blood cell counts ($<4.0\times10^9$/l), and hypofibrinogenemia (<2.5 g/l). The diagnosis of MAS requires the presence of two or more of these criteria.

For the diagnosis of EBV-HLH, EBV load in peripheral blood was quantified by real-time PCR as described in our previous study [28]. Patients were diagnosed as having EBV-HLH if they had EBV loads of over 1,000 genome copies per milliliter in whole blood and fulfilled the diagnostic criteria used in the HLH-94/HLH-2004 Study.

A total of 82 patients, 39 males and 43 females, were enrolled in the present study. Among the 82 patients, 48, including 33 having systemic JIA with MAS, were diagnosed as having secondary HLH at Yokohama City University Hospital between November 2000 and December 2009. The remaining 34 patients, who were diagnosed as having secondary HLH between March 2007 and December 2010, were registered in the HLH-2004 as a study of Japanese Pediatric Leukemia/Lymphoma Study Group. In these patients, 32 were diagnosed as having EBV-HLH. The 188 control subjects were recruited from apparently healthy adult volunteers.

Notably, the 33 MAS patients were identical to those analyzed in our previous study, where the significance of *IRF5* polymorphisms was evaluated among systemic JIA patients with or without MAS. In this study, to evaluate the significance of *IRF5* polymorphisms in the susceptibility to secondary HLH as a whole, data were reanalyzed in comparison with healthy controls using the different study population.

This study was performed in accordance with the Declaration of Helsinki and approved by the Ethics Committee of the Yokohama City University School of Medicine and each member of the Japan Leukemia/Lymphoma Study Group. Written informed consent was obtained from each patient or his/her guardians as well as the control subjects.

Table I Characteristics entire secondary HLH Study Group and subgroups

	N	Age	Gender
All patients with secondary HLH	82	4.7 (1–16)	39 (47.6%)
Subgroups of HLH patients			
MAS	33	4.8 (1–16)	16 (48.5%)
Non-MAS HLH	49	4.6 (1–15)	23 (46.9%)
EBV-HLH	32	4.3 (1–15)	16 (50.0%)

HLH hemophagocytic lymphohistiocytosis, *MAS* macrophage activation syndrome, *Non-MAS HLH* secondary HLH including EBV-HLH but not MAS, *EBV-HLH* Epstein–Barr virus-associated HLH

Genotyping

Three SNPs—rs729302, rs2004640, and rs2280714—in the *IRF5* gene were selected as described in our previous study [21]. Patients with HLH and control subjects were genotyped using TaqMan SNP Genotyping Assays as described previously [21].

Statistical Analysis

The SNPassoc package using R-language, version 2.8 (The R Foundation for Statistical Computing, http://www.R-project.org) was employed to evaluate the associations between HLH and the SNPs by logistic regression analysis [29]. Haplotype phases and haplotype frequencies were estimated using the Expectation–Maximization algorithm as implemented in the haplostat package (minimum haplotype frequency, >0.05; www.docstoc.com.) [30]. The associations between genotypes under study and laboratory values were analyzed by the Jonckheere–Terpstra test. The following laboratory values were included: levels of hemoglobin, neutrophils, platelets, triglycerides, fibrinogen, ferritin, transaminases, and lactate dehydrogenase. The association between HLH and the *IRF5* haplotypes was evaluated by logistic regression analysis.

Results

Patient characteristics are summarized in Table I. The mean age of the 82 patients with secondary HLH was 4.7 years (1–16 years) at onset. The numbers of patients with MAS and non-MAS HLH were 33 and 49, respectively. In those with non-MAS HLH, 32 with EBV-HLH were included.

The genotype frequencies for the three SNPs of the HLH patients, including their subgroups, and the control subjects were in Hardy–Weinberg equilibrium ($p>0.05$). These results were consistent with the findings of a recent Japanese population study (Table II) [31].

Table II Association of polymorphisms in the *IRF5* gene with susceptibility to secondary HLH

SNP subject subset	*n*	MAF	Allelic association			
			OR	(95% CI)	*p* value	p_c
		rs729302				
All patients with secondary HLH	82	0.20	1.05	0.96–1.15	0.26	n.s.
Subgroups of HLH patients						
MAS	33	0.18	1.04	0.96–1.12	0.32	n.s.
Non-MAS HLH	49	0.20	1.03	0.95–1.12	0.46	n.s.
EBV-HLH	32	0.23	1.00	0.93–1.10	0.90	n.s.
Control subjects	188	0.24	1.0	–	–	
		rs2004640				
All patients with secondary HLH	82	0.49	0.88	0.82–0.95	<0.01	0.006
Subgroups of HLH patients						
MAS	33	0.50	0.92	0.86–0.99	0.02	n.s.
Non-MAS HLH	49	0.49	0.91	0.84–0.98	0.01	0.030
EBV-HLH	32	0.55	0.95	0.88–1.01	0.11	n.s.
Control subjects	188	0.35	1.0	–	–	
		rs2280714				
All patients with secondary HLH	82	0.34	1.1	1.02–1.19	0.02	0.0465
Subgroups of HLH patients						
MAS	33	0.32	1.07	1.00–1.14	0.06	n.s.
Non-MAS HLH	49	0.35	1.07	0.99–1.14	0.09	n.s.
EBV-HLH	32	0.36	1.04	0.98–1.12	0.22	n.s.
Control subjects	188	0.44	1.0	–	–	

IRF5 interferon regulatory factor 5, *SNP* single nucleotide polymorphism, *MAF* minor allele frequency (the C allele at rs729302, T rs2004640, C rs2280714), p_c corrected combined *p* value using the Bonferroni method